Al-Nahrain Journal for Engineering Sciences

Al-Nahrain J. Eng. Sci. 29(1) 47-56, 2026
Original Article

Surface modification of 316L Stainless Steel alloy using Nano Ceramic Hydroxyapatite, Magnesium Oxide, Zinc Oxide, and composite coating by EPD to enhancing corrosion resistance in biomedical application

Aya Muhsin Hazber[1]●, Ayad Naseef Jasim[2] and Abbas Al-Bawee[3]●.

1,2,3 Department of Material, College of engineering, University of Diyala, Baquba, Iraq

●*These authors contributed equally to this work*

DOI: http://doi.org/10.29194/NJES.29010047

Received: March 22, 2025 **Revised:** June 8, 2025 **Accepted:** July 16, 2025 **Published:** March 20, 2026

Abstract

The toxicity of permanent implants is the main concern. The release of ions from the substrate leads to toxicity. Because of how the human body works biologically, the toxicity of corrosion compounds is a byproduct of wear and fretting debris. aimed to improve the corrosion resistance of a 316L stainless steel substrate. Bio ceramic Nano-hydroxyapatite (HA) was coated using the Electrophoretic Deposition (EPD) technique. Stainless steel has good mechanical properties and high compatibility, but it suffers from body fluid attack due to its chloride content, which can penetrate the passivation layer, resulting in the release of chromium and nickel ions. Tissues and organs are damaged by the ions and debris that are released. To address this problem, it was coated with bioceramic using the EPD method. Suspensions of various powders—hydroxyapatite, magnesium oxide, zinc oxide, and the composite—were prepared and coated by electrophoretic deposition. The coated samples were dried at room temperature to ensure a homogeneous coating structure. The zeta potential test for magnesium oxide and hydroxyapatite suspensions was positive, while zinc oxide and complex suspensions were negative. One of the important parameters for achieving electrolyte and implant balance is the open circuit potential (OCP). A substantial change towards a more noble direction (less negative) was seen in the OCP-coated (316 L) alloy, suggesting excellent thermodynamic stability. Tafel extrapolation analysis was used to obtain the corrosion potential (Ecorr) and corrosion current density (Icorr) values of composite-coated stainless steel 316L, which are generally derived from the polarization curve. The findings that are in line with the MgO, HA, and ZnO coatings show a significant decrease in corrosion current (Icorr), an increase in corrosion potential (Ecorr), and a decrease in corrosion rate from (4.386×10^{-1} mm/y) Stainless Steel 316 L to (1.417×10^{-2} mm/y) MgO Coated and (1.222×10^{-3} mm/y) (65%MgO+25%ZnO+10%HA coated).

Keywords: *Corrosion, Polarization Curve, Hydroxyapatite, Bioceramic, Metallic Implants, Electrophoretic Deposition EPD.*

Corresponding author: Provide the corresponding author information and publisher here. E-mail address: engayo53@gmail.com

1. Introduction

An artificial implant made of metal is one example of a material used by the human body. Orthopedic implants typically utilize stainless steel alloys; however, 316L stainless steel, known for its high mechanical strength, is the most commonly used variety in orthopedic implants [1][2],[3],[4]. When choosing metals and alloys for use in living organisms, corrosion must be considered. As a result of corrosion, the body may be exposed to allergenic, toxic/cytotoxic, or carcinogenic species. Implant loosening and eventual failure can also be caused by different mechanisms of corrosion. In most cases, the lack of osteoconductive in metallic implants makes it difficult for the implant to adhere to the surrounding tissue, using biopolymers to make biomedical coatings. suggests processing and coating flexibility with respect to temperature. [5],[6]. The non-toxicity, antibacterial activity, biodegradability, biocompatibility, and hemostatic properties of chitosan, a naturally occurring cationic biopolymer, make it an ideal candidate for use in biomedical applications. Particular modifications are possible thanks to its structure, which eliminates a lot of issues. On the other hand, chitosan isn't without its drawbacks; building bone takes a long time, and crosslinkers are essential for keeping the structure intact [7]. Body devices made of metal have been covered with hydroxyapatite (HA) because it is biocompatible, bioactive, and chemically similar to the inorganic part of bone tissue[8]. It was possible to make biopolymer and Bioceramic layers that were a good mix when

chitosan and hydroxyapatite were placed together. This will lead to bones that look like human bones. In general, chitosan made the best link between the substrate and the layer coating. It also works great as a binder for layer components [9] [10]. Hydroxyapatite (HA) is one of the Bioceramic that has been studied the most because it is chemically close to the mineral part of bone. Bioactive, biocompatible, and thermodynamically stable in body fluid are some of the other qualities that make it an important material for many uses in biomedical areas. Also, hydroxyapatite (Ha)(Ca10(PO4)6(OH)2) was looked at as a possible replacement for bones and teeth because it has similar chemical makeup to natural apatite and can be biocompatible with muscle, skin, and hard tissues. It also bonds directly to bones without harming cells [11] Hydroxyapatite can't be used in many situations because it has weak or bad mechanical properties. So, to fix this issue, Ha needs to be applied to the metal surface [12]. The second bio ceramic material are Bioactive zinc oxide (ZnO) has great potential as a Bioceramic coating for stainless steel 316L. It increases the bioactivity of hydroxyapatite composites, promotes bone formation, and displays antibacterial activity when added in different quantities [13], [14]. In biomedical applications, ZnO coatings can increase stainless steel's corrosion resistance and make osseointegration easier [15]. The coated alloy is more biocompatible and has better mechanical stability thanks to the addition of ZnO, which makes it a good candidate for use in medical devices such as implants. Thirdly, magnesium oxide (MgO) is being used more and more as a coating material for Bioceramic because of its useful qualities in biomedical fields. It promotes bone growth and integration by increasing the mechanical stability and biological activity of implants. Orthopedic implant biodegradable magnesium alloys can benefit from MgO coatings, which increase biocompatibility and corrosion resistance [16] [17][18]. And because of its magnesium ion-releasing properties, MgO promotes osteoblast development and speeds up the healing process. [17] [19]. Chitosan is a natural cationic polysaccharide that has many useful properties, including the ability to kill microbes, being biocompatible, and having improved mechanical and other properties that have been used in biomedical implants and drug delivery [20]. The widely recognized electrodynamic phenomenon known as electrophoresis is the building block of electrophoretic deposition (EPD). Various materials have been prepared and deposited using the EPD approach for thick films throughout the past hundred years [21] [22]. Electrophoresis with particle migration (EPD) involves applying a uniform DC electric field to a liquid medium, which causes the particles to migrate and deposit on one of the two electrodes. Organic macromolecules can also be separated using electrophoresis-based techniques[23]. Despite this, EPD offers a number of benefits over previously documented coating methods, such as being able to achieve its results at ambient temperature.[24] Electrophoretic deposition is economical since it involves minimal infrastructure and supplies only the necessary equipment [25]. The metallurgical, geometrical, mechanical, and chemical properties of the solution environment are the many factors that contribute to the complicated multi-factorial phenomena known as corrosion. In order for any metal to be used in surgical devices, corrosion must be avoided first. Biomaterial contains any natural or man-made substance that interacts with living things and/or biological processes [26]. The bio-corrosion, bioactivity, and osteointegration properties of implant materials in relation to the physiological environment must be understood in relation to medical implants [27]. Also, osteointegration is weak on metallic surfaces since they aren't bone bioactive. Adding hydroxyapatite [Ca10(PO)6(OH)2] to metallic implants makes them more bioactive to bone. Bioceramic hydroxyapatite mimics the mineral coating of natural bone and tooth tissue [28]. In this study, we will use an electrophoretic deposition technique to coat a stainless steel 316L alloy with a single layer of nano hydroxyapatite (HA), nano magnesium oxide (MgO), nano zinc oxide (ZnO), and a composite layer. We will then examine the biocorrosion behavior and corrosion resistance of this coated alloy in an SBF solution.

2. Experimental work

2.1 Materials

1-316L stainless steel used as the substrate has the chemical composition listed in Table 1.

2-Bio-ceramic (Hydroxyapatite, Magnesium Oxide, Zinc Oxide) less than 40 nm purchased from Sky Spring Nanomaterials, USA.

3-(Deionized water, solvents of ethanol absolute (99.9%), and acetic acid with purity (99.5%)).

Table 1. Chemical composition of 316L stainless steel

Sample	C%	Si%	Mn%	P%	S%	Cr%	Mo%	Ni%	Cu%	Al%	Fe%
Used %	0.0273	0.467	1.40	0.0296	<0.0005	17.36	2.14	11.9	0.431	0.0042	Ball
Standard (ASTM)	0.03	0.75	2	0.04	0.03	16-18	2	10-14	–	–	Remain

2.2 Sample preparation

The electrode plates made of stainless steel 316L were first wire-cut to the dimensions (10 x 20 x 3 mm) and (17 x 17 x 3 mm), as illustrated in Figure (1). After that, the electrode plates were ultrasonically cleaned for an hour using ethanol and acetone, in that order. The plates were dehydrated before the electrophoretic coating technique. Here, electrophoretic deposition (EPD) was used to create every coating. Two electrodes were submerged in the coating suspension in the beaker that served as the electrophoretic deposition cell for this study. Both the working and counter anodes were made of the stainless steel 316L substrate. The constant distance between them when submerged in suspension was 10 mm. The electrodes were dehydrated and then washed with acetone. To carry out the deposition, the electrode was submerged in a beaker containing the coating material suspension. A 316L stainless steel

substrate was coated using an electrophoretic deposition device, as shown in Figure 2. Throughout the trials, varying coating times were used, given that the digital timer was used to establish the required duration for every experiment. In addition, the electrodes were raised and lowered electrically, and they were fixed according to the design basis for the cell deposition regime.

In electrodeposition (EPD) technology, the main function of applied voltage is to generate an appropriate electric field that attracts positively charged Tau particles in suspension to an electrode that has an opposite charge. leading to their accumulation on the surface of the medicinal layer. Particle motion and deposition rate are both affected by the electric field strength, which is in turn determined by the applied direct current (DC) voltage. The deposition rate, as well as the thickness and shape of the deposited layer, can be altered by increasing the voltage. The thickness and amount of material deposited onto the substrate can be controlled by adjusting the time in the Electrophoretic Deposition (EPD) process.

A thicker and denser coating is produced as the EPD process progresses due to the accumulation of charged particles that migrate towards the electrode. The length of time an electric field is applied has a direct impact on the rate of deposition and the ultimate properties of the film. The shape, homogeneity, and functional qualities of the coating can be precisely controlled by adjusting the deposition time. Electrophoretic Deposition (EPD) is greatly affected by the particle concentration in the suspension in terms of the deposition rate. Because there are more charged particles to migrate and deposit onto the substrate under the applied electric field, the deposition rate is often increased when the particle concentration is higher. The end product is a coating that is thicker and heavier with the same amount of deposition time.

(a) (b)

Figure 1. shows Stainless Steel 316L (a) square shape (b)rectangular shape

3. Invitro Test

3.1 Zeta potential

The electrophoretic mobility distributions of the entire suspension were evaluated in relation to zeta potential utilizing particle electrophoresis equipment. in order to guarantee uniform coating thickness and stable colloidal suspension. The zeta potential shows whether the coating layers were deposited cathodically or anodically. Before testing, each sample was diluted in a specific liquid to make sure the suspension.

The zeta potential test was conducted at room temperature using a device made by Brookhaven Instruments called Zeta Plus, which is located in the USA. This evaluation took place in the Science and Technology Ministry. A thirty-minute ultrasonic processing followed by magnetic stirring was performed on the suspension prior to testing. Measuring was then carried out.

3.2 Microstructural examination

This method was applied to describe the surface. Scanning electron microscopy (SEM) was used to assess the cross-sectional microstructures and the distribution of the various coating components. The elemental distribution of the chosen points/area in the SEM image was found using an Energy Dispersive X-ray Spectrometry (EDS) detector in conjunction with SEM. This test was Conducted in Al Khora Company.

3.3 Corrosion Test Results

Specimen corrosion in SBF was demonstrated by electrochemical measurements taken with a potentiostat/galvanostatic on both coated and untreated samples. (Chinese Electrochemical CHI 604 e Corr Test bed). The samples were evaluated using a 650 mL multiport corrosion cell kit in accordance with ASTM G1-03 and ASTM G5-94 standards. In the past, three electrodes were used: a reference electrode made of saturated calomel (SCE), a counter electrode made of platinum platelet, and the working electrode, which was the specimen itself. The corrosion rate is evaluated using the mpy technique with the following Equation 1:

$$[CR] = [0.13 \times i\text{corr} \times \frac{EW}{D}] \quad \ldots\ldots\ldots(1)$$

where: Icorr: The current density of corrosions (mA.cm-2), and CR: The corrosion rate (mpy). Efficiency of protection (PE%) of each composite coating layer is calculated using the following formulas:

$$[PE\%]=[\frac{(Icorr)\ uncoated - (Icorr)\ coated}{(Icorr)\ uncoated}]x100\% \ldots\ldots\ldots(2)$$

Here, Icorr (coated) represents the inhibited corrosion current density and Icorr (uncoated) represents the uninhibited current density.

4. Result and Discussion

4.1 Zeta Potential test

The stability of coated suspensions was investigated using the zeta potential method. The results demonstrate that all acidic suspensions exhibited positive zeta potential values. Since the pH of the suspensions has a significant impact on the zeta potential, it is an essential consideration. All of the suspensions had their pH values changed to make them more stable, and the result was dense, uniform layers of composite coating. When the pH is low, the zeta potential is positive; when the pH is high, it is negative These results are consistent with the researcher.[29]. The electrical charge that reaches the surface of particles in colloidal solutions with a high zeta potential is greater, enhancing the particles' electrostatic attraction. Colloidal solutions that have a low ζ potential, on the other hand, attempt to clump together or coagulate, this agrees with the researcher [30]. In order to get a uniform composite coating, the interaction between the charges of the positive and negative materials is crucial. put another way, the capacity of materials with

positive charges to encircle materials with negative charges by attracting them to cathodic deposition. A positive zeta potential and mobility were shown in the single layer coating of HA, MgO, indicating that the zeta potential deposition was cathodic. As for the single layer of ZnO, as well as the composite coating layers of (HA+MgO+ZnO), both the zeta potential and mobility were negative, indicating that the deposition was anodic, as shown in Figure 2 and Table (2).

Table 2. Demonstrates principles Single and composite layer Zeta potential

Type of Coating	Zeta Potential (mV)	Mobility
Hydroxyapatite	25.70	2.01
Magnesium Oxide	24.65	1.93
Zinc Oxide	-33.85	-2.64
65% HA+25% MgO +10% ZnO	-74.10	-1.47
65% MgO +25% ZnO +10% HA	-86.97	-1.73
65% ZnO +25%HA +10% MgO	-63.12	-1.25

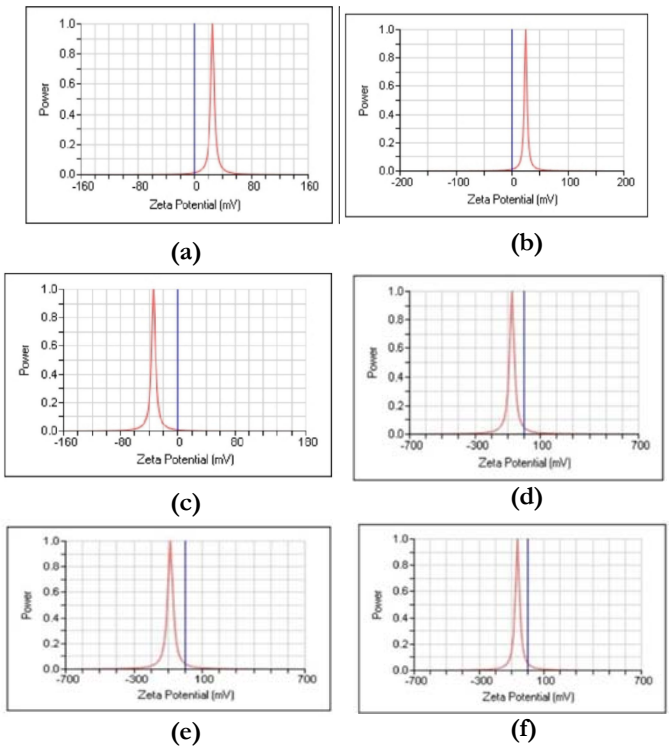

Figure 2. Shows Values of Zeta potential of **(a)** HA **(b)** MgO **(c)** ZnO **(d)** 65% HA+25% MgO +10% ZnO **(e)** 65% MgO +25% ZnO +10% HA **(f)** 65% ZnO +25%HA +10% MgO

4.2. Scanning electron microscopy (SEM) results

The surface layer structure for the composite coating single coating was determined using SEM Figure 3 shows that the uniform dispersion of particles led to a uniform coating. When magnified at a great level Coatings made by Molaei et al. had no surface flaws or holes because they contained chitosan, an active binder, these results that are consistent with what the researcher obtained [31]. Stable suspensions give the impression of a more consistent and homogeneous coating surface. The most stable suspensions are those with the highest zeta potential values, which is consistent with this theory and supported by observations in coated materials, as also confirmed by the researcher [32]. On the zeta potential dependent, the following parameters can impact coating quality when using the EPD process: Duration of deposition, voltage applied, suspension concentration [33], the sample's current, the age of the suspension and the stability of the suspension. All of the aforementioned elements had a considerable impact on the coating's performance, however It was significantly [34], and the stability of the suspension. All of the aforementioned elements had a considerable impact on the coating's performance, however. It was significantly impacted by the zeta potential. These results are consistent with the researchers' [33,34 and 35].

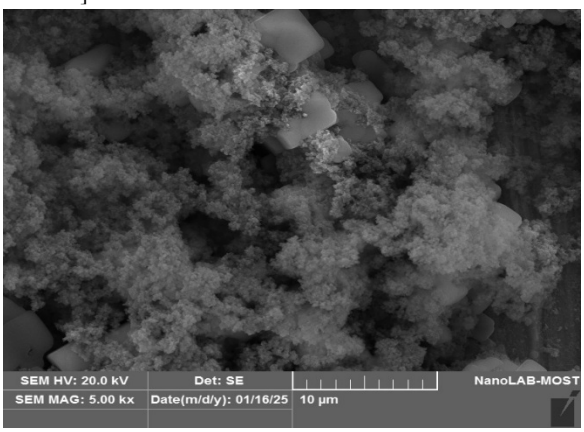

Figure 3. Shows SEM of (a) Single Coating layer (MgO), (b) multilayer composite coating (65% MgO + 25% ZnO+ 10% HA)

4.3. Electrochemical bio-corrosion

The toxicity of permanent implants is the main concern. When ions are released from the substrate, toxicity occurs. Because of how the human body works biologically, the toxicity of corrosion compounds is a byproduct of wear and fretting debris. Nonimplant able and implantable medical devices consistently utilize the 316L SS substrate due to its excellent corrosion resistance. Because of its ionic nature, the human body's biological milieu is hostile to metals. Another issue with metallic alloys in humans is wear debris. Tissues and organs are damaged by the ions and debris that are released. The coating process is one way to protect metals and their alloys from the harsh environments found in human bodies. Both the untreated substrate and the biopolymer composite covering have had their polarization curves examined. Corrosion decreased with the addition of layers of biopolymer single and composite coating, as seen in Table 3 where the corrosion rate decreased for the uncoated 316L stainless steel sample compared to the coated sample with the single

layer and composite coating layer; this means the corrosion rate decreased with the single and composite coating layer than the uncoated sample. Also, it can be noticed from this table that the open-circuit potential (OCP) value decreased for the uncoated 316L stainless steel sample compared with single and composite layers coated sample. Additionally, the corrosion rate decreased from the coated sample with the composite coating layer. suggesting that the coated sample becomes less active. The base, or uncoated sample, exhibits a rather large hysteresis loop. The discussion could be enhanced by deeper comparisons with related literature and more critical interpretation of the results (AL-Ali et al., 2024; Al-Bawee et al., 2025; El-Bassyouni et al., 2025; Khethier Abbass et al., 2020) [36,37, 38, and 26].

Table 3. Corrosion test results for 316L stainless steel alloys (uncoated and coated) in both single- and composite-layer configurations

Sample	OCP (V)	E corrosion (V)	I corrosion (Amp)	Corrosion rate (mmpy)	E rep (V)
Stainless Steel 316 L	-0.528	-0.168	1.491*10 -5	4.386×10^{-1}	0.203
Zno Coated	-0.384	-0.221	6.810 *10 -6	2.003×10^{-1}	0.302
Ha Coated	-0.236	-0.062	3.528 *10 -6	1.037×10^{-1}	0.776
Mgo Coated	-0.120	-0.208	4.820 * 10 -7	1.417×10^{-2}	-ve loop
65%Zno+25%Ha+10%Mgo coated	-0.219	-0.495	1.231×10^{-7}	3.621×10^{-3}	-ve loop
65%Ha+25%Mgo+10%Zno Coated	-0.088	-0.284	8.207×10^{-8}	2.414×10^{-3}	-ve loop
65%Mgo+25%Zno+10%Ha coated	0.112	-0.446	4.155×10^{-8}	1.222×10^{-3}	-ve loop

5.Open Circuit Potential (OCP) measurement

One of the important parameters for achieving electrolyte and implant balance is the open circuit potential (OCP). Immersing the samples in SBF solution and monitoring their OCP for 30 minutes allowed them to reach a steady-state potential. Figure 4 shows the open circuit potential (OCP) of a 316L alloy substrate that has no coating and three different coatings —HA, Mgo, and Zno, and composite layer coating. Obtaining the OCP value from these curves As compared with uncoated 316L alloy was (OCP = -0. 528V) and single layer (Zno -OCP=-0.384),(OCP-Ha = -0. 236V), (Mgo-OCP = -0.120V) . A substantial change towards a more noble direction (less negative) was seen in the OCP-coated (316 L) alloy, suggesting excellent thermo-dynamic stability. After immersing 316L alloy, HA, Mgo, and Zno single-layer coated layers in SBF. Table 4 displays the results of open circuit potential (OCP). There was a considerable rise in the ratio of EOCP to coated samples as compared to the uncoated 316L sample, indicating that the coated samples are less prone to corrosion. The coated materials' characteristics that lessen corrosion through raising the potential are consistent with these findings. In the second part of the work we applied three layers of coating (composite coats) and the OCP value 65% Mgo + 25% Zno+ 10% HA Coated (0.112 V),OCP of 65% Ha+25% Mgo +10% Zno Coated (-0.088 V) and OCP of 65%Zno +25%HA +10% Mgo coated (-0.219 V) was . This finding proves that the Zno, Ha, and Mgo coatings effectively reduced corrosion on the stainless steel surface by forming a protective layer.

The open circuit voltage value of 65% Mgo+ 25% ZnO+ 10% HA (0.112V) obtained a positive value, indicating that the composite coatings were superior to the single coating layer. This indicates that the coating significantly increases the corrosion resistance of the implants, as all of them have a higher noble corrosion potential than the uncoated sample.

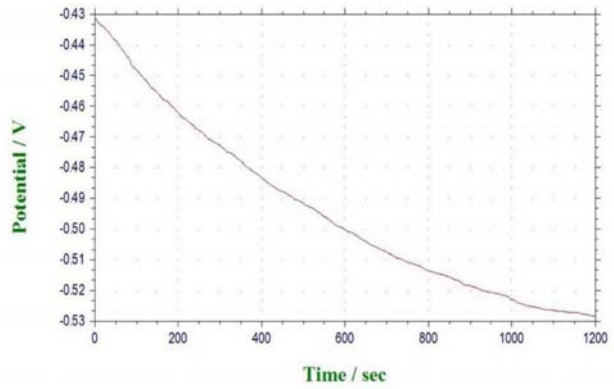

(a)

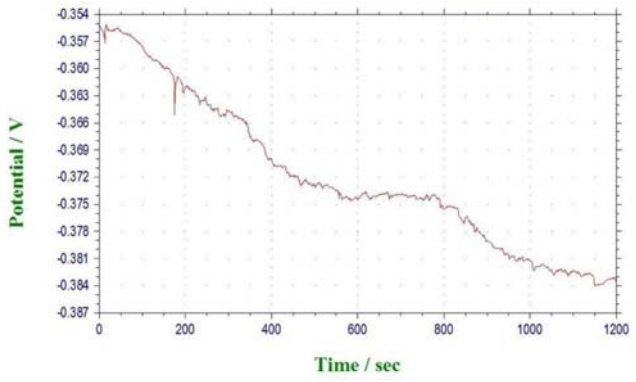

(b)

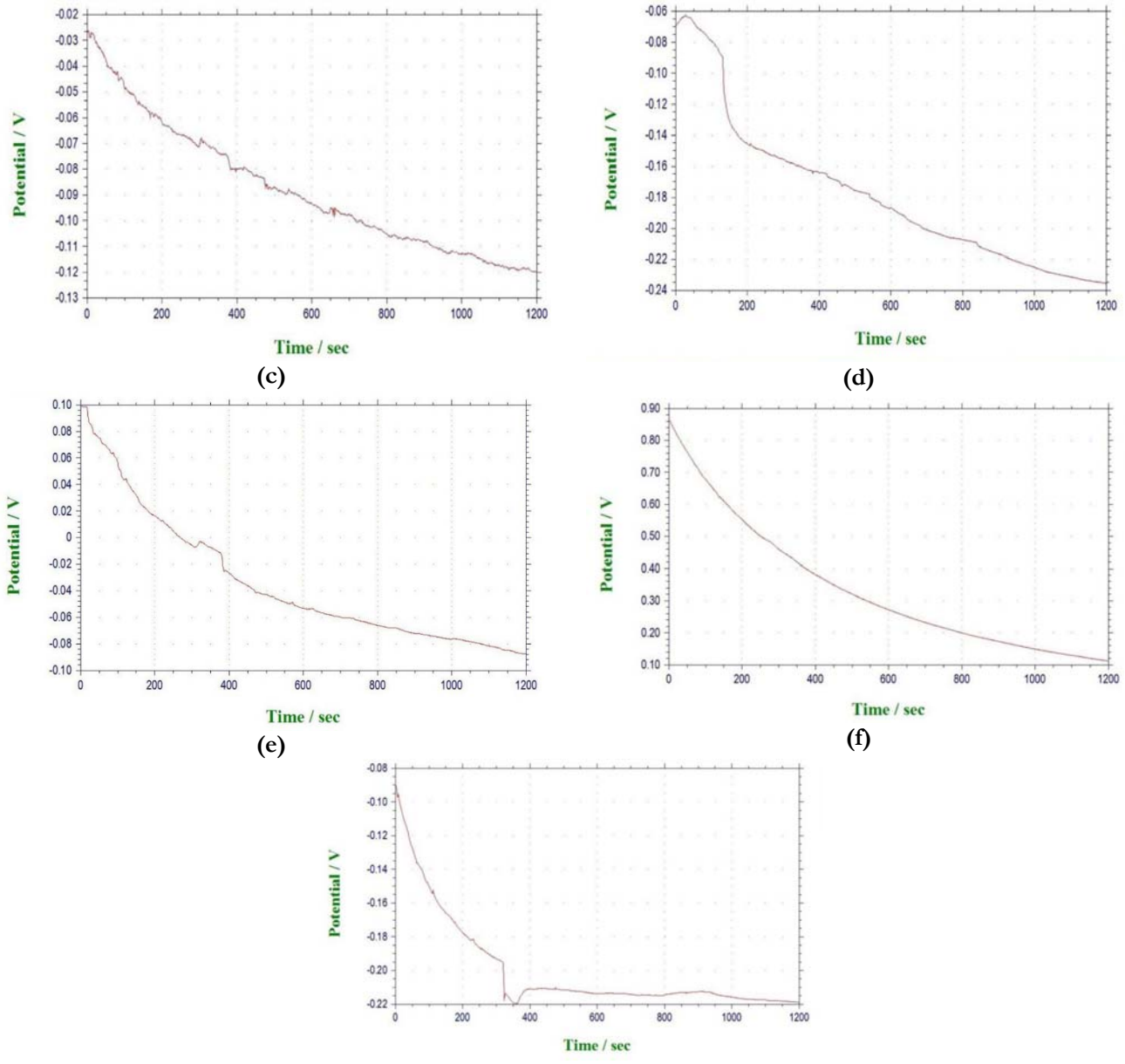

Figure 4. Display Open Circuit Potential (OCP) of single and composite layer coating of (a) Stainless steel 316 L without coat (b) ZnO coated (c) MgO coated, (d) HA coated, (e) 65% HA+ 25% MgO+ 10%ZnO coated, (f) 65% MgO + 25% ZnO+ 10% HA coated and (g) 65% ZnO +25%HA +10% MgO coated.

Table 4. shows the results of (open circuit potential) OCP of an uncoated (316L) alloy, and single and Composite Layers after immersion in SBF

Type Of Specimens	OCP(V)
Stainless Steel 316 L	-0.528
ZnO	-0.384
HA	-0.236
MgO	-0.120
65%ZnO +25%HA +10% MgO coated	-0.219
65% HA+25% MgO +10% ZnO	-0.088
65% MgO + 25% ZnO+ 10% HA	0.112

6.Potentiodynamic polarization (Tafel Extrapolation)

The specimens in the SBF solution are depicted in Figure (5) together with their potentiodynamic polarization curves. Apart from that, the corrosion parameters, which were modified from the polarization curves using the extrapolation Tafel method. Tafel extrapolation analysis was used to obtain the corrosion potential (Ecorr) and corrosion current density (Icorr) values of composite-coated Stainless steel 316L, which are generally derived from the polarization curve. Data from corrosion experiments are shown in Table 5, for HA-single layer, MgO-single layer, and ZnO-single layer. The findings that are in line with the MgO, HA, and ZnO coatings shown a significant decrease in corrosion current (Icorr), an increase in corrosion potential (Ecorr), and a decrease in corrosion rate. The

coating creates a barrier layer on the substrate, which makes it different from untreated 316L stainless steel, induced a decrease in electrochemical corrosion resistance which In addition, the discrepancies found in the corrosion current density (Icorr) value with respect to 316L alloys that have been composite coated, which show that the coating is protective, however the corrosion current density is significantly reduced due to the HA single layer coating (3.528*10-6)(μA/cm2) ,MgO single layer (4.820*10-7) and ZnO single layer (6.810*10-6) in comparison to Stainless Steel 316L substrate (1.491*10-5 mA/cm2) is This is due to the fact that the coating layer likely provides protection and the corrosion potential of MgO covered is moved toward higher values. (-0.120 V) (-0.236 V) ,MgO coated value (-0.236 V) ,and ZnO coated value (-0.384 v)in comparison to the Stainless Steel 316L substrate (−0.528 V). All of the specimens coated with MgO, HA, or ZnO had lower anodic current densities than the 316L stainless steel specimens. While the current density in Composite Coating layer 65% MgO + 25% ZnO+ 10% HA Coated are (4.155*10 -8 μA/cm2) , 65% HA+25% MgO +10% ZnO (8.207 *10 -8 μA/cm2) and 65%ZnO +25%HA +10% MgO coated (1.231 *10 -7 μA/cm2) Depending on the exact composition and environmental factors, the open circuit potential (OCP) of composite layers including hydroxyapatite, magnesium oxide, and zinc oxide might differ from one layer to the next. Composite layers have better corrosion resistance than uncoated substrates and coating single layer because their values are often lower. This is because the layers are more compact and there is less porosity. The significance of the coating's composition and structure in affecting electrochemical performance is highlighted by this phenomenon.

Table 5. Displays the corrosion test results for both uncoated and coated stainless steel 316 L, including both single- and multi-layer coatings.

Type of Specimens	I corr (μA/cm²)	E corr (V)	Corrosion rate (mpy)
Stainless steel 316 L	1.491 *10 -5	-0.168	4.386 *10 -1
Zno Coated	6.810 *10 -6	-0.221	2.003 *10 -1
Ha Coated	3.528 *10 -6	-0.062	1.037 *10 -1
Mgo Coated	4.820 *10 -7	-0.208	1.417 *10 -2
65%Zno+25%HA+10% Mgo coated	1.231 *10 -7	-0.495	3.621 *10 -3
65%Ha+25%Mgo+10% Zno	8.207 *10 -8	-0.284	2.414 *10 -3
65% Mgo + 25% Zno+ 10% HA	4.115 *10 -8	-0.446	1.222 *10 -3

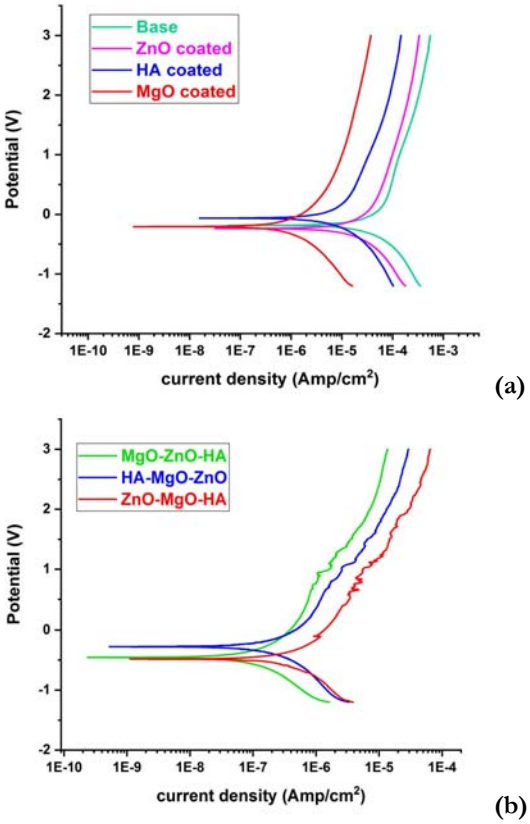

Figure 5. Tafel Extrapolation curves of: (a)uncoated Substrateand and single coated layer (b) Cyclic polarization curves of composite coating layers

7.Cyclic Polarization

Corrosion parameters, taken from cyclic curves, listed in Table 6 and Figure 6. Corresponding results of coated samples with (HA, MgO and ZnO) single layer, and Composite layers indicate a considerable reduction in corrosion as well as an increase in the potential.

Table 6. Shows Potential of Repassivation for the uncoated alloy Stainless steel 316 L and coated in single and composite layer

ITEM E rep

ITEM	E rep
Base	0.203
ZnO coated	0.302
HA coated	0.776
MgO coated	-ve loop
65%ZnO +25%HA +10% MgO coated	-ve loop
65% HA+25% MgO +10% ZnO	-ve loop
65% MgO + 25% ZnO+ 10% HA	-ve loop

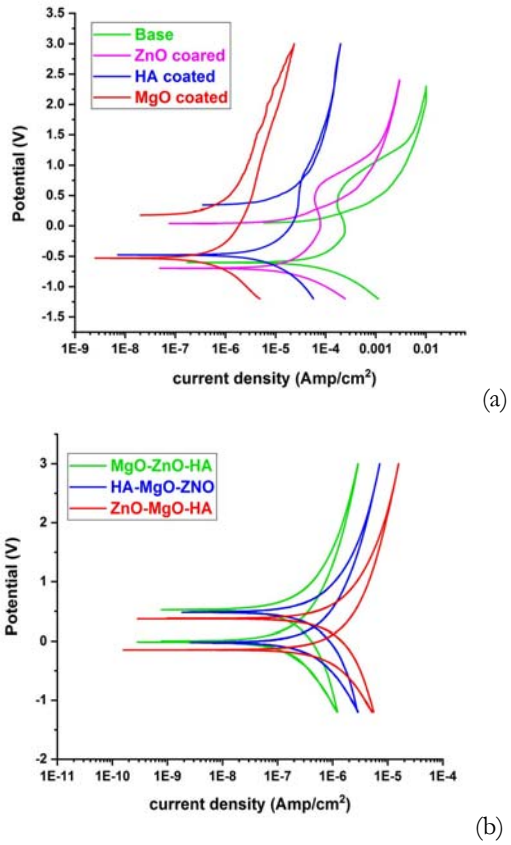

Figure (6): Cyclic polarization curves of: (a)uncoated Substrate and single coated layer (b) Cyclic polarization curves of composite coating layers

8.Conclusions

Positive zeta potential and mobility were shown in the single layer coating of HA, MgO, indicating that the zeta potential deposition was cathodic,

Negative zeta potential and mobility were shown in the single layer coating of ZnO indicating that the zeta potential deposition was anodic.

Both the zeta potential and mobility were negative in composite layer, indicating that the deposition was anodic.

A open-circuit potential of the substantial change towards a more noble direction (less negative) was seen in the OCP-coated (316 L) alloy, suggesting excellent thermo-dynamic stability.

Decrease in corrosion current (Icorr), with increase in corrosion potential (Ecorr), and a decrease in corrosion rate, the coating creates a barrier layer on the substrate.

The findings that are in line with the MgO, HA, and ZnO coatings shown decrease in corrosion rate from (4.386 × 10-1 mm/y) Stainless Steel 316 L to (1.417 × 10-2 mm/y) Mgo Coated and (1.222 × 10-3 mm/y) (65%MgO+25%ZnO+10%HA coated.

9.References

[1] K. Ceyhun and R. Kacar, "In vitro bioactivity and corrosion properties of laser beam welded medical grade AISI 316L stainless steel in simulated body fluid," Int. J. Electrochem. Sci., vol. 11, no. 4, pp. 2762-2777, 2016.
https://doi.org/10.1016/S1452-3981(23)16139-6

[2] S. B. Goodman, Z. Yao, M. Keeney, and F. Yang, "The future of biologic coatings for orthopaedic implants," Biomaterials, vol. 34, no. 13, pp. 3174-3183, 2013.
https://doi.org/10.1016/j.biomaterials.2013.01.074

[3] H. T. Aro, J. J. Alm, N. Moritz, T. J. Mäkinen, and P. Lankinen, "Low BMD affects initial stability and delays stem osseointegration in cementless total hip arthroplasty in women: a 2-year RSA study of 39 patients," Taylor & Francis, 2012.
https://doi.org/10.3109/17453674.2012.678798

[4] A. G. Gristina, "Biomaterial-centered infection: microbial adhesion versus tissue integration," Science, vol. 237, no. 4822, pp. 1588-1595, 1987.
https://doi.org/10.1126/science.3629258

[5] Z. C. Wang, F. Chen, L. M. Huang, and C. J. Lin, "Electrophoretic deposition and characterization of nano-sized hydroxyapatite particles," J. Mater. Sci., vol. 40, no. 18, pp. 4955-4957, 2005.
https://doi.org/10.1007/s10853-005-3871-x

[6] A. Balamurugan, G. Balossier, J. Michel, and J. M. F. Ferreira, "Electrochemical and structural evaluation of functionally graded bioglass-apatite composites electrophoretically deposited onto Ti6Al4V alloy," Electrochim. Acta, vol. 54, no. 4, pp. 1192-1198, 2009.
https://doi.org/10.1016/j.electacta.2008.08.055

[7] A. Stoch, A. Brożek, G. Kmita, J. Stoch, W. Jastrzębski, and A. Rakowska, "Electrophoretic coating of hydroxyapatite on titanium implants," J. Mol. Struct., vol. 596, no. 1-3, pp. 191-200, 2001.
https://doi.org/10.1016/S0022-2860(01)00716-5

[8] T. Matsushita and H. Takahashi, "Orthopedic applications of metallic biomaterials," in Metals for Biomedical Devices, Elsevier, 2019, pp. 431-473.
https://doi.org/10.1016/B978-0-08-102666-3.00017-1

[9] Z. Zhang, T. Jiang, K. Ma, X. Cai, Y. Zhou, and Y. Wang, "Low temperature electrophoretic deposition of porous chitosan/silk fibroin composite coating for titanium biofunctionalization," J. Mater. Chem., vol. 21, no. 21, pp. 7705-7713, 2011.
https://doi.org/10.1039/c0jm04164e

[10] S. Heise et al., "Electrophoretic deposition and characterization of chitosan/bioactive glass composite coatings on Mg alloy substrates," Electrochim. Acta, vol. 232, pp. 456-464, 2017.
https://doi.org/10.1016/j.electacta.2017.02.081

[11] M. A. Hussain et al., "Mechanical properties of CNT reinforced hybrid functionally graded materials for bioimplants," Trans. Nonferrous Met. Soc. China, vol. 24, pp. s90-s98, 2014.
https://doi.org/10.1016/S1003-6326(14)63293-3

[12] S. Mahmoodi, L. Sorkhi, M. Farrokhi-Rad, and T. Shahrabi, "Electrophoretic deposition of hydroxyapatite-chitosan nanocomposite coatings in different alcohols," Surf. Coat. Technol., vol. 216, pp. 106-114, 2013.
https://doi.org/10.1016/j.surfcoat.2012.11.032

[13] E. Abd Al-Majeed and O. S. Mahdi, "Preparation and characterization bioactive properties of bioceramic composite (Zinc Oxide/Hydroxyapatite)," J. Eng. Appl. Sci., vol. 14, pp. 9504-9508, 2019.
https://doi.org/10.36478/jeasci.2019.9504.9508
[14] W. G. Billotte, D. B. Reynolds, G. M. Mehrotra, R. Srinivasan, and P. K. Bajpai, "In vitro characterization of a zinc based bioceramic," Biomed. Sci. Instrum., vol. 33, pp. 126-130, 1997.
[15] S. Sadeghzade, R. Emadi, and F. Tavangarian, "Synthesis of silicate zinc bioceramic via mechanochemical technique," in Advances in Powder and Ceramic Materials Science, Springer, 2020, pp. 143-150.
https://doi.org/10.1007/978-3-030-36552-3_15
[16] M. Nabiyouni, T. Brückner, H. Zhou, U. Gbureck, and S. B. Bhaduri, "Magnesium-based bioceramics in orthopedic applications," Acta Biomater., vol. 66, pp. 23-43, 2018.
https://doi.org/10.1016/j.actbio.2017.11.033
[17] A. Saberi, M. S. Baltatu, and P. Vizureanu, "Recent advances in magnesium-magnesium oxide nanoparticle composites for biomedical applications," Bioengineering, vol. 11, no. 5, p. 508, 2024.
https://doi.org/10.3390/bioengineering11050508
[18] N. Azarian and S. M. M. Khoei, "Characteristics of a multi-component MgO-based bioceramic coating synthesized in-situ by plasma electrolytic oxidation," J. Magnes. Alloys, vol. 9, no. 5, pp. 1595-1608, 2021.
https://doi.org/10.1016/j.jma.2020.12.018
[19] M. Razavi, M. Fathi, O. Savabi, L. Tayebi, and D. Vashaee, "Biodegradable magnesium bone implants coated with a novel bioceramic nanocomposite," Materials, vol. 13, no. 6, p. 1315, 2020.
https://doi.org/10.3390/ma13061315
[20] M. H. Abdulkareem, A. H. Abdalsalam, and A. J. Bohan, "Influence of chitosan on the antibacterial activity of composite coating (PEEK/HAp) fabricated by electrophoretic deposition," Prog. Org. Coat., vol. 130, pp. 251-259, 2019.
https://doi.org/10.1016/j.porgcoat.2019.01.050
[21] L. Besra and M. Liu, "A review on fundamentals and applications of electrophoretic deposition (EPD)," Prog. Mater. Sci., vol. 52, no. 1, pp. 1-61, 2007.
https://doi.org/10.1016/j.pmatsci.2006.07.001
[22] F. Hossein-Babaei and B. Raissi-Dehkordi, "Fabrication of poly-Si thick films by electrophoretic deposition," Electron. Lett., vol. 37, no. 17, pp. 1090-1092, 2001.
https://doi.org/10.1049/el:20010723
[23] M. G. Khaledi, High Performance Capillary Electrophoresis, vol. 146, John Wiley & Sons, Inc., New York, pp. 303-401, 1998.
[24] M. Farrokhi-Rad, "Electrophoretic deposition of hydroxyapatite nanoparticles in different alcohols: effect of Tris (tris (hydroxymethyl) aminomethane) as a dispersant," Ceram. Int., vol. 42, no. 2, pp. 3361-3371, 2016.
https://doi.org/10.1016/j.ceramint.2015.10.130
[25] A. Michelmore, "Thin film growth on biomaterial surfaces," in Thin Film Coatings for Biomaterials and Biomedical Applications, pp. 29-47, 2016.
https://doi.org/10.1016/B978-1-78242-453-6.00002-X
[26] M. K. Abbass, A. N. Jasim, M. Jasim, K. S. Khashan, and M. J. Issa, "Improving bio corrosion resistance of the single layer of nano hydroxyapatite and nano YSZ coating on the Ti6Al4V alloy using electrophoretic deposition," Solid State Technol., vol. 63, no. 6, pp. 18584-18597, 2020.
[27] J. Chen, J. G. C. Wolke, and K. De Groot, "Microstructure and crystallinity in hydroxyapatite coatings," Biomaterials, vol. 15, no. 5, pp. 396-399, 1994.
https://doi.org/10.1016/0142-9612(94)90253-4
[28] H. Zeng and W. R. Lacefield, "XPS, EDX and FTIR analysis of pulsed laser deposited calcium phosphate bioceramic coatings: the effects of various process parameters," Biomaterials, vol. 21, no. 1, pp. 23-30, 2000.
https://doi.org/10.1016/S0142-9612(99)00128-3
[29] D. Li, "Microfluidic methods for measuring zeta potential," Interface Sci. Technol., vol. 2, pp. 617-640, 2004.
https://doi.org/10.1016/S1573-4285(04)80032-2
[30] D. Predoi, S. L. Iconaru, M. V. Predoi, M. Motelica-Heino, R. Guegan, and N. Buton, "Evaluation of antibacterial activity of zinc-doped hydroxyapatite colloids and dispersion stability using ultrasounds," Nanomaterials, vol. 9, no. 4, p. 515, 2019.
https://doi.org/10.3390/nano9040515
[31] A. Molaei, M. Yari, and M. R. Afshar, "Modification of electrophoretic deposition of chitosan-bioactive glass-hydroxyapatite nanocomposite coatings for orthopedic applications by changing voltage and deposition time," Ceram. Int., vol. 41, no. 10, pp. 14537-14544, 2015.
https://doi.org/10.1016/j.ceramint.2015.07.170
[32] O. Saleem, M. Wahaj, M. A. Akhtar, and M. A. Ur Rehman, "Fabrication and characterization of Ag-Sr-substituted hydroxyapatite/chitosan coatings deposited via electrophoretic deposition: a design of experiment study," ACS Omega, vol. 5, no. 36, pp. 22984-22992, 2020.
https://doi.org/10.1021/acsomega.0c02582
[33] İ. Aydın, A. I. Bahçepınar, M. Kırman, and M. A. Çipiloğlu, "HA coating on Ti6Al7Nb alloy using an electrophoretic deposition method and surface properties examination of the resulting coatings," Coatings, vol. 9, no. 6, p. 402, 2019.
https://doi.org/10.3390/coatings9060402
[34] A. Wu, P. M. Vilarinho, and A. I. Kingon, "Electrophoretic deposition of lead zirconate titanate films on metal foils for embedded components," J. Am. Ceram. Soc., vol. 89, no. 2, pp. 575-581, 2006.
https://doi.org/10.1111/j.1551-2916.2005.00732.x
[35] A. N. Jasim, Enhancing the mechanical properties and biological characteristics of EPD nano composites functionally graded organic-inorganic systems for medical applications, M.Sc. thesis, Dept. Prod. Eng. Metall., Univ. Technol., Baghdad, Iraq, 2020.
[36] A. Al-Bawee, Z. T. Khodair, and A. K. Hussein, "Impact of surface titanium alloy coatings for biomedical applications," in AIP Conf. Proc., AIP Publishing, 2025.
https://doi.org/10.1063/5.0265031
[37] G. T. El-Bassyouni, S. M. Mouneir, and A. M. El-Shamy, "Advances in surface modifications of titanium and its alloys:

implications for biomedical and pharmaceutical applications," Multiscale Multidiscip. Model. Exp. Des., vol. 8, no. 5, p. 265, 2025. https://doi.org/10.1007/s41939-025-00823-1

[38] A. Al-Ali, M. H. Abdulkareem, and I. A. Anoon, "Antibacterial improvement with multilayer of bio-composite coatings produced by electrophoretic deposition," Eng. Technol. J., vol. 42, no. 1, pp. 1-12, Jan. 2024. https://doi.org/10.30684/etj.2023.143475.1588